

# **Influence of limestone aggregate on mortars for repair and replacement of old buildings' renders**

Yunuén Delgado Huaracha

Instituto Superior Técnico, Universidade de Lisboa

May 2018

---

## **1. Introduction**

The deterioration of old building renders and the need to preserve the existing masonries leads to the development of adequate mortar solutions that can better respect the compatibility between the different materials and simultaneously assure the mechanical, aesthetic and durability performance. Traditional renders applied in old buildings are essentially lime-based mortars. The application of these mortars has been progressively replaced by cement mortars, including for restoration of old masonry structures. Cement-based mortars enable higher mechanical strengths and lower setting times. However, it has been found that the use of such mortars in old buildings leads to various degradation mechanisms in existing elements and accelerates global deterioration (Veiga, 2003; Stefanidou & Papayianni, 2005). In these cases, an adequate choice of mortar is essential and due to the greater similarity with the rendering mortars in old buildings, air lime mortars allow a better overall performance of the replacement and repair elements (Veiga, 2005; Moropoulou, et al., 2009). The poor mechanical strength development and reduced durability of these mortars has limited their application. The influence of the aggregate type on the mechanical behavior of air lime mortars has been investigated, aiming at improving knowledge in this domain. Aggregates being the most representative component in mortars significantly influence their structure and behavior. Regarding the incorporation of different aggregate types, some studies indicate that the mechanical strength tends to be higher when siliceous sands are replaced by calcareous aggregates in traditional mortars (Lanas & Alvarez, 2003; Scannell, et al., 2014; Vysvaril, et al., 2017). The mechanical strength improvement has been mainly attributed to the better quality achieved at the aggregate-paste interface zone. In fact, it has been suggested that the higher angularity and porosity of crushed limestone sands enhance the bond with the hardened paste, ultimately increasing the mechanical strength. At the same time, because of the better chemical compatibility between the aggregates and the binder (both of calcite nature), the nucleation of calcite crystals formed during carbonation is favorable and a more cohesive and regular interface region is obtained (Lanas & Alvarez, 2003).

The increasing use of lime-based mortars for restoration of old buildings, allied to the loss of manufacture and application techniques, justifies their further research. This dissertation aimed to study the influence of the incorporation of limestone aggregate on the physical and mechanical behavior of air lime mortars used in old building renders. To this end, 5 mortars with different proportions of crushed limestone aggregates, in substitution of the more traditional siliceous sands, were produced. The different mortars were tested in the fresh and hardened state to evaluate properties for the adequate performance of old buildings' repair and replacement mortars. Complementary tests were defined to study the aggregate-paste bond with the different aggregate types.

## 2. Experimental Program

### 2.1. Materials

The experimental program involved the physical and mechanical characterization of 5 aerial lime mortars. The aggregate mixture was different in each mortar. Two different types of fine aggregates were used: a natural siliceous sand aggregate (SS) and a crushed limestone aggregate (CS). The siliceous sands used in the experimental program are made up of round shaped particles and have quartz as the main component, whereas the limestone aggregate is characterized by angular shape and irregular texture and shows calcite at very high percentages (96%±3%). The grading curve concerning the particle size distribution of the siliceous aggregate was determined by the sieving method, in accordance with EN 933-1. The reference grading curve was matched for the limestone to minimize the influence of the particle size distribution in the results, after initially separating the aggregate by particle size using the same method. In all tested mortars, a 1:2,5 binder to aggregate volume ratio was used. The same water/binder ratio was adopted on 4 of the mortars. The w/b ratio was established by determining the amount of water required to obtain a suitable workability measured by flow table test (160±15 mm). The 4 mortars had different ratios of each aggregate in the mixture, namely was used 0, 50, 75 and 100% of limestone sand in different mortars (C0A, C50, C75 and C100 respectively). Since it was not possible to obtain the appropriate workability for the 100% siliceous mortar, an additional mortar was produced with 0% of the calcareous sand in the mixture in which a lower w/b ratio was adopted, so that it presented a similar workability as established initially (C0E). In all compositions a CL-80 aerial lime was used. The proportions of the components used on the different mortars are in Table 1.

Table 1 – Mix proportions

Mortar	C100	C75	C50	C0A	C0E
w/b	1,25	1,25	1,25	1,25	1,05
SS (g/dm <sup>3</sup> )	-	378,4	742,7	1431,7	1506,0
CS (g/dm <sup>3</sup> )	1402,9	1032,1	675,2	-	-
Lime (g/dm <sup>3</sup> )	252,5	247,7	243,1	234,3	246,4
Water (g/dm <sup>3</sup> )	315,6	309,6	303,8	292,9	258,8

### 2.2. Methods and curing

The 5 different mortars were tested in the fresh and hardened state to evaluate properties for the adequate performance of old buildings' repair and replacement mortars. In addition, 2 of the compositions (C100 and C50) were tested at different ages (28, 60, 90 and 120 days) to evaluate the development of carbonation and of the physical and mechanical properties. The table flow, density and water retention tests were adopted for the fresh state characterization. The hardened state tests considered on the experimental program were the evaluation of compressive and flexural strength, hardened density and open porosity, ultrasound and modulus of elasticity, as resumed in Table 2. The dimension adopted for the test specimens was 160x40x40mm, in accordance with EN 1015-2. Samples were cured in dry chamber (T=20<sup>0</sup>±5<sup>0</sup> C; HR=50±5%) and tested after 120 days of curing. Modulus of elasticity and axial tensile tests were settled at 150 days. For each composition at each curing stage 3 different specimens were tested on similar conditions.

Table 2 – Tests considered on the hardened state

Test	Standard	Specimen	Compositions studied	Curing
Flexural strength	EN 1015-11	160x40x40	5	Dry chamber (RH=50% T=20°C)
Compressive strength	EN 1015-11	80x40x40		
Ultrasound	EN 12504-4	160x40x40		
Open porosity	RILEM I.1	80x40x40		
Hardened density	RILEM I.2	80x40x40		
Modulus of elasticity	EN 1052-1	160x40x40	2	
Axial tensile strength	-	40x40x40		

Complementary axial tensile tests and tensile aggregate-paste bonding tests were carried on a Lloyd LR50K to study the bond at the aggregate-paste interface with the different aggregate types. For this purpose, 2 types of samples were produced: cubes of 40x40x40mm according to EN 1015-11 for C100 and C50 mortars; non-traditional specimens with a resin base, seen in Fig. 1 (40x40x40mm). For the nontraditional specimens used in the aggregate-paste bonding tests, a resin prism with 160x40x20mm was initially produced in which selected aggregates of the natural siliceous or the crushed limestone sands were incorporated at the surface before hardening. After sectioning the hardened prism in 4 smaller specimens of 40x40x20mm, a layer of fresh mortar was applied and compacted over the resin. The specimens were stored in dry chamber with 5% of carbon dioxide concentration after demolding. To determine the adherence strength, according to the maximum recorded force in the tensile test, an EINSCAN-PRO scanner from Shinings3D and CATIA software were used to design a topographic level map for the assessment of the aggregate area in contact with the hardened paste. For the complementary tests, 5 cube specimens were tested for each different composition (C100 and C50) and 5 for the non-traditional specimens.



Fig. 1 – Specimens for the aggregate-paste bond tests

### 3. Results and discussion

#### 3.1. Fresh state properties

##### 3.1.1. Workability

Lower workability was obtained when higher proportions of limestone aggregate were used in the mixes due the crushed particles being more angular and elongated, creating higher surface areas and increasing friction. For the 100% siliceous sand mortar (C0E), it was necessary to increase the amount of water in 20% to obtain a similar workability as C100 mortars.

##### 3.1.2. Fresh density and air content

The density of mortars was lower when higher proportions of crushed limestone sand were used since the angularity of the particles increases friction and hinders the particle organization, resulting in less

compact mixes. Associated with that, higher air content and paste volumes were obtained in those compositions, which also contributed to the decrease in density. C0E mortars presented higher density due to the lower w/b ratio, resulting in lower air content and paste volumes.

### 3.1.3. Water retention

All mortars showed water retention higher than 90%, with only C0A mortars showing inferior results. As suggested by the fluid consistency of C0A mortars, there was higher amount of free water not adsorbed by the aggregate in the mixes, which was rapidly lost the in the fresh state. The water retention increased when higher ratios of limestone were incorporated due to the shape and texture of the aggregates, which need more added water to obtain the required workability. At the same time, the higher overall porosity of limestone aggregates, due to the presence of calcite, leads to an increase in water absorption.

Table 3 - Fresh state properties

	<b>C100</b>	<b>C75</b>	<b>C50</b>	<b>C0A</b>	<b>C0E</b>
<b>Flow table (mm)</b>	145	161	173	200	145
<b>Density (kg/m<sup>3</sup>)</b>	2034	2056	2060	2107	2111
<b>Water retention (%)</b>	97,2	94,9	93,2	87,6	96,0
<b>Air content (%)</b>	5,72	4,54	4,25	1,76	4,11
<b>Paste volume (%)</b>	44,4	44,1	43,4	42,9	38,9

## 3.2. Hardened state properties

### 3.2.1. Compressive and flexural strength

In general, the compressive and flexural strength of the tested mortars was lower than 0,50MPa and 1,0MPa, respectively, a range considered compatible with old building renders (Veiga, 2005). The mortars with higher percentages of limestone aggregate achieved higher strength. These results are according with the findings from previous studies, that limestone aggregates can produce stronger mortars in comparison with the more traditional mixes with siliceous sands (Nogueira, 2016; Lanás & Alvarez, 2003; Scannell, et al., 2014; Vysvaril, et al., 2017). However, an approximate range of mechanical strength was obtained by all mortars except for percentages of limestone aggregate higher than 75% in the mixture. In fact, for C100 mortars, an increase of 31% in flexural strength and 38% in compressive strength was obtained in comparison with the mortars with the same w/b ratio with siliceous sand (C0A), while regarding the remaining mortars with the same w/b ratio, the increase in compressive and flexural strength was 21-24% and 32-35% for 50% and 75% of incorporation of the crushed limestone sand, respectively. In comparison with the mortars with a lower w/b ratio with siliceous sand (C0E), an increase of 24% and 35% was registered, for compressive and flexural strength correspondingly. The analysis of the failure mode of the mortars suggested modifications developing in the aggregate-paste interface zone, which ultimately are considered responsible for the different mechanical performance. As seen in Fig. 2 and Fig. 3, the specimens with limestone aggregate showed a more homogeneous failure, with less aggregate visible at the surface. The calcareous particles, when visible, showed paste still attached to the surface. The opposite occurred when the natural silicate sand was used, where the aggregates surface was clearly visible. In that regard, the analysis of the failure mode of the different mortars showed contribution of different regions of the mortar structure. A stronger aggregate-paste bond when limestone was used in higher proportions enabled a larger contribution of

the binder and the failure developed through the paste matrix, whereas the weaker bond controlled the failure of mortars where siliceous aggregates were used. In fact, a better bond can be obtained because the angular shape, irregular texture and higher global porosity of the limestone aggregate increase adherence at the interface region. In addition, the limestone aggregates have a similar calcitic matrix as the binder, providing nucleating sites for the crystal growth at the interface during carbonation (Lanas & Alvarez, 2003). At the same time, due to the elastic compatibility between lime and limestone aggregates, microcracking decreases in the interface region (Yildirim & Sengul, 2011). These factors contribute to enhance the quality at the aggregate-paste interface zone, increasing strength since that bond controls mechanical resistance in air lime mortars. In accordance with the importance of the interface, C0E compositions developed less strength than C100 mortars despite the lower w/b ratio.



Fig. 2 – Failure of C100 specimen (10.4x ampliation)

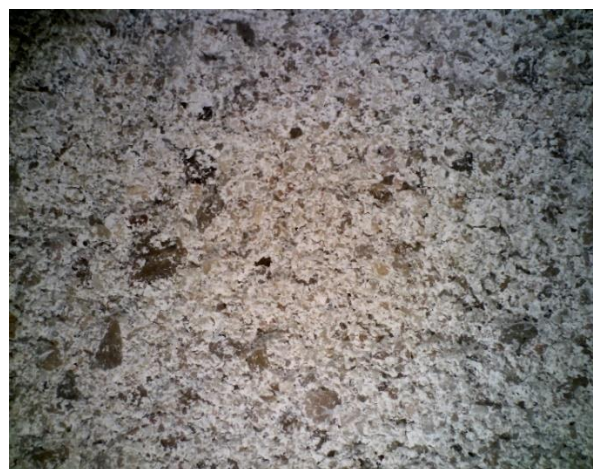


Fig. 3 – Failure of C0A specimen (10.4x ampliation)

Table 4 – Mortars characteristics at 120 days

	<b>C100</b>	<b>C75</b>	<b>C50</b>	<b>C0A</b>	<b>C0E</b>
<b>Compressive strength (MPa)</b>	1,12	0,85	0,83	0,81	0,90
<b>Flexural strength (MPa)</b>	0,58	0,42	0,41	0,39	0,37
<b>Open porosity (%)</b>	27,7	27,3	26,1	24,7	23,7
<b>Hardened density (kg/m<sup>3</sup>)</b>	1853	1869	1866	1916	1937
<b>V<sub>US</sub> (m/s)</b>	1525	1440	1444	1437	1555
<b>E<sub>d</sub> (MPa)</b>	3792	3488	3502	3560	4215
<b>E<sub>s</sub> (MPa)</b>	834	-	1109	-	-
<b>Axial tensile strenght (MPa)</b>	0,16	-	0,15	-	-

Table 5 – Mortar characteristics at different curing stages

	<b>28 days</b>		<b>60 days</b>		<b>90 days</b>		<b>120 days</b>	
	<b>C100</b>	<b>C50</b>	<b>C100</b>	<b>C100</b>	<b>C100</b>	<b>C50</b>	<b>C100</b>	<b>C50</b>
<b>Compressive strength (MPa)</b>	0,43	0,35	0,74	0,66	1,08	0,79	1,12	0,83
<b>Flexural strength (MPa)</b>	0,28	0,28	0,33	0,35	0,51	0,41	0,58	0,41
<b>Carbonation depth (mm)</b>	3,8	1,5	6,5	6,3	11,8	11,6	20,0	20,0
<b>Open porosity (%)</b>	28,7	27,2	28,2	27,2	28,1	26,2	27,7	26,1
<b>Hardened density (kg/m<sup>3</sup>)</b>	1834	1848	1850	1865	1857	1891	1853	1871

The same tendency was observed in the specimens tested at different curing stages in which the mortar with a higher percentage of the crushed limestone sand on the aggregate mixture (C100) had higher

flexural and compressive strength at all tested ages than C50 mortars. The difference in performance was more evident after 90 days, when the depth of carbonation reached is more important.

### **3.2.2. Evolution of carbonation**

Phenolphthalein staining was used to determine the depth of carbonation in specimens from C100 and C50 mortars at different curing stages. At 28 days, samples from C100 were more carbonated than C50 specimens. Since air lime mortars gain strength with the diffusion of carbon dioxide through carbonation, the higher strength of the mix with calcareous sand may be attributed to the higher level of carbonation at that stage. The efficiency of the penetration is attributed to the higher porosity of C100 mortars. After 2 months of curing the samples from the different mixes showed identical levels of carbonated area but C50 had achieved less strength. Because of that, the better mechanical performance was not attributed to the rate of carbonation but to the aggregate-paste interface zone quality, as suggested by the analysis of the failure mode. At 120 days, only C0E mortars did not show the samples totally carbonated.

### **3.2.3. Porosity and hardened density**

The more porous and less dense mortars were produced with higher proportions of crushed limestone sand. The angularity and irregularity of the crushed limestone particles increase friction and hinder the compaction of the mixes. In that cases, the lower workability also contributed to a reduction in the compactness as did the higher volume of paste. C0E mortars, produced with lower w/b ratio, presented lower porosity. Contrary to what is normally observed in hydraulic binder mortars, the more porous and lower density mortars had better mechanical characteristics. In fact, despite being less compact, mortars with limestone reached higher strength, enhancing the importance of the interface zone in the mechanical behavior of air lime mortars. At the same time, the higher porosity of these mortars eased the drying process and benefited the penetration of carbon dioxide and accelerated carbonation when calcareous sand was incorporated in higher proportions, namely during the first 2 months of lime hardening. Coherent with the evolution of carbonation, C50 and C100 mortars tested at different curing ages showed a decrease in the porosity during the period of testing. At all tested stages, C100 presented higher porosity and lower density for the same reasons previously discussed.

### **3.2.4. Ultrasound**

The ultrasound measurements were close for all the different tested mortars. Ultrasound velocity is essentially related to the hardened density and the elasticity of the mortars' components and of the aggregates in particular that are the most representative in the mixture. On one hand, quartz present in the siliceous aggregate is harder than calcite that constitutes limestone and an increase in  $V_{us}$  is expected when incorporating siliceous aggregate. At the same time, paste and air content was higher when crushed limestone sand was used and, since more porous mortars tend to associate with lower ultrasound results, the same tendency was expected in the ultrasound test results. On the other hand, limestone aggregate used in this study had higher density than the natural siliceous sands available ( $CS=2700\text{kg/m}^3$  and  $SS=2600\text{kg/m}^3$ ). Because these factors counterbalance, the results were very close for all mortars with the same w/b, excluding C100 mortars. Regarding C100, Arizzi et al. (2013) suggest that a better cohesion at the aggregate-paste interface reduces the attenuation of the wave resulting in higher  $V_{us}$ . The mechanical characterization and the analysis of the failure mode of the different mortars showed modifications happening at the interface and a better bond when limestone

aggregate was incorporated, particularly for C100 mortars. Nevertheless, such substantial increase was not predictable. Expectedly, in the composition with a lower w/b relation (C0E) the ultrasound velocity was superior by significantly altering one phase of the mortar by reducing w/b.

### 3.2.5. Modulus of elasticity

The dynamic modulus of elasticity ( $E_d$ ) was determined for all mortars according to Eq. (1).

$$E_d = V_{US}^2 \rho \frac{(1 + \nu_d)(1 - 2\nu_d)}{(1 - \nu_d)} \quad (1)$$

As expected,  $E_d$  followed the same tendency as  $V_{US}$ , in accordance with the proportions of the different aggregate types and the adopted w/b ratio. The results point toward the higher deformability of mortars with limestone aggregate which is mainly attributed to the lower rigidity of calcite and the higher volume of paste in those mortars (the same factors affecting  $V_{US}$ ). However, contrary to the evolution of the parameter, C100 had higher  $E_d$  than the other mortars with the same w/b ratio. The enhanced quality at the aggregate-paste interface, which increased  $V_{US}$ , affected the results.

The static modulus of elasticity ( $E_s$ ) was determined for C100 and C50 mortars by the secant of the stress-strain curve between 20% and 60% of the average compressive strength of the mortars at 120 days. The specimens were subjected to 10 loading cycles (compression) and the test was carried on INSTRON as seen in Fig. 4. The deformation of the specimens was evaluated by using 2 deflectometers.



Fig. 4 – Test scheme to estimate the static modulus of elasticity

As suggested by the tendency of the estimated  $E_d$  for the tested mortars,  $E_s$  for mortars with a 50-50 ratio of the different sands was higher than the value obtained for C100 mortars. However, due to the composite and non-linear behavior of mortars, the estimated values for  $E_d$  were invariably higher than  $E_s$ . Mortars are low resistance quasi-brittle materials and their deformability is also conditioned by the properties of the interface region. In low strength mortars, as air lime-based mortars, the elastic incompatibility between the aggregates and the surrounding matrix is greater than in cement-based mortars and, because of that, the aggregate-paste transition zone becomes more susceptible to the formation and development of microcracks during loading (Nogueira, 2016; Yildirim & Sengul, 2011). Only the determination of  $E_s$  by destructive test is sensitive to microcracking, whereas the estimation of

$E_d$  according to the ultrasound test is determined in non-cracked conditions, resulting in the underestimation of  $E_s$ . The development of microcracking is expectedly less relevant when limestone aggregate is used because of the elastic compatibility between the aggregate and the hardened paste. In contrast, the hard quartz present in the siliceous sand increases the heterogeneity at the interface resulting in a worse composite behavior. In fact, in the analysis of the stress-strain curves, as exemplified in Fig. 4, 2 separate linear sections can be distinguished: the first linear section corresponding to stress values between 0,2 and 0,7 of the reference compressive strength at 120 days and the second to 0,7 and 0,9 of that value. In the first section, corresponding to the slope used to estimate  $E_s$ , C100 shows a higher deformability mainly due to the lower stiffness of the constituents, calcite in particular. However, in the second section there is an inversion in the stiffness of the mortars, which is according to a lesser development of microcracking in the interface zone of C100 that allowed a better composite behavior. This indicates a better-quality aggregate-paste bond as also suggested by the mechanical characterization and the analysis of the different failure modes.

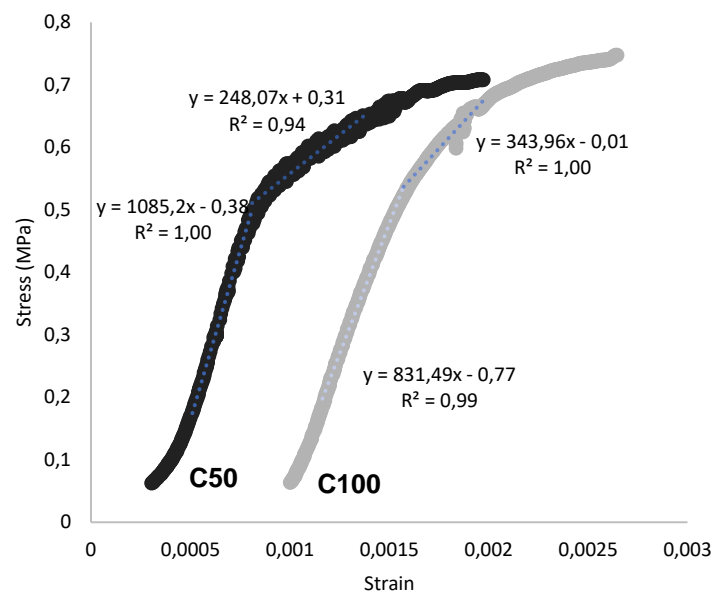


Fig. 1 – Example of stress-strain curve of compressive loading used to estimate  $E_s$

### 3.3. Complementary tests for characterization of the aggregate-paste interface

#### 3.3.1. Axial tensile test

The mortar where limestone sand was used in a higher ratio (C100) showed a marginally higher traction strength than C50. Nevertheless, the results for the different compositions tested were very similar and the variability in the results was high. The high variability in the results is attributed to the limitations inherent to the realization of tensile tests, specifically the alignment of the load with the specimen at all times during the test to prevent the development of secondary bending moments. Also, after the formation of the first crack, the crack development does not happen throughout the section instantaneously. In fact, after the first crack initiates, part of the load starts to be supported by the non-cracked region, generating a secondary moment that leads to the early rupture of the specimen. Tensile tests are also very susceptible to differences in leveling between the top and bottom of the specimens that may generate a stress gradient and lead to an underestimation of strength values. Since the

aggregate-paste bond is the weaker region in mortars, the tensile tests were developed to give indication of the quality of the interface zone. However, due to the inherent limitations of the test and the high variability of the results, the slight increase in C100 mortars is not considered conclusive regarding the enhanced quality of the aggregate-paste interface region. Nevertheless, the analysis of the failure mode of the tested specimens confirmed the observations of the mechanical characterization, with the limestone aggregates showing paste still attached to the surface and C50 having a less homogeneous and regular rupture in comparison with C100 specimens.



Fig. 5 – Axial tensile test scheme

**3.3.2. Aggregate-paste bonding test**

The test results indicate similar adherence strength for the different aggregate types, contrary to what was showed in the mechanical characterization tests. However, similarly to what was discussed in the previous section, the aggregate-paste bonding tests on the special specimens were not conclusive since it was difficult to guarantee the uniform distribution of tensile stress in the section and the variability in the results was high. In addition, the low resistance of the specimens only enabled 5 valid results (2 with limestone aggregate and 3 with siliceous aggregate). The test was also considerably influenced by the characteristics of the different aggregates. Due to the more elongated and flattened shape of the limestone sand particles, the aggregate area in contact with the paste was considerably lower for the same number of particles incorporated. As such, the adherence force in the tensile test was lower for the specimens with limestone aggregate, leading to early ruptures of the samples.

Table 6 - Results of the aggregate-past bond tests

	<b>Aggregate area (mm<sup>2</sup>)</b>	<b>Adherence strength (MPa)</b>
<b>Specimens with limestone aggregates</b>	47,67	0,141
	100,03	0,266
<b>Specimens with siliceous aggregates</b>	332,6	0,422
	164,33	0,185
	393,1	0,214

#### 4. Conclusions

In general, the mechanical characterization of the tested mortars corroborates the tendency verified in previous studies, in which the incorporation of limestone aggregates enabled the mortars to achieve higher strength. In fact, an increase in compressive and flexural strength was observed for mortars produced with higher ratios of limestone sand, particularly for incorporations higher than 75%. Even regarding mortars of similar workability, the use of limestone aggregate in a mortar with a w/b ratio 20% superior than the mortar with siliceous sand, lead to an increase in flexural and compressive strength. The better performance in those cases was attributed to the better characteristics at the aggregate-paste interface zone, as suggested by the analysis of the failure mode. The better connection was mainly enabled by the irregular texture and higher porosity of limestone sands and the elastic and chemical compatibility between the hardened paste and the aggregates. The incorporation of siliceous aggregate lead to failure developing preferably in the interface region whereas mortars with limestone, capable of developing better quality transition zones, lead to higher mechanical strength with failure developing preferably in the paste. These phenomena showed higher importance in the mechanical behavior of mortars than the fact that mortars with crushed limestone sand presented lower compactness. The use of less rigid and more compatible limestone aggregates also enabled mortars to have a better composite behavior leading to higher deformability. Also, carbonation developed faster in mortars with limestone aggregate particularly during the first 2 months of curing. The increased porosity in mortars with limestone facilitated drying and the penetration of carbon dioxide, accelerating the development of the reactions.

#### References

- Arizzi, A., Martínez-Martínez, J. & Cultrone, G., 2013. Ultrasonic wave propagation through lime mortars: an alternative and non-destructive tool for textural characterization. *Materials and Structures*, Volume 46, pp. 1321-1355.
- Lanas, J. & Alvarez, J., 2003. Masonry repair lime-based mortars: Factors affecting the mechanical behavior. *Cement and Concrete Research*, Volume 33, pp. 1867-1876.
- Moropoulou, A., Bakolas, A., Moundoulas, P. & Aggelakopoulou, E., 2009. Reverse engineering: a proper methodology for compatible restoration of mortars. Em: *Workshop Repair of Mortars of Historic Masonry*. s.l.:Rilem Publications, pp. 278-291.
- Nogueira, R., 2016. "Lime plasters and renders. Characterization and assessment of consolidation treatments". *Thesis to obtain PhD Degree in Civil Engineering*. Lisboa: IST.
- Scannell, S., Lawrence, M. & Walker, P., 2014. Impact of aggregate type on air lime mortar properties. *Energy Procedia*, Volume 62, pp. 81-90.
- Stefanidou, M. & Papayianni, I., 2005. The role of aggregates on the structure and properties of lime mortars. *Cement and Concrete Composites*, Volume 27, pp. 914-919.
- Veiga, M. d. R., 2003. *Argamassas para revestimento de paredes de edificios antigos. Características e campo de aplicação de algumas formulações correntes*. Lisboa, LNEC.
- Veiga, M. d. R., 2005. *Comportamento de rebocos para edificios antigos: Exigências gerais e requisitos específicos para edificios antigos*. Lisboa, LNEC.
- Vysvaril, M., Zizlavsky, T. & Bayer, P., 2017. The effect of aggregate type on the properties of lime mortars. *Applied Mechanics and Materials*, Volume 861, pp. 141-148.
- Yildirim, H. & Sengul, O., 2011. Modulus of elasticity of substandard and normal concretes. *Construction and Building Materials*, Volume 25, pp. 1645-1652.